

Self-Rewarded Multimodal Coherent Reasoning Across Diverse Visual Domains

Jesen Zhang¹, Ningyuan Liu¹, Kaitong Cai¹, Sidi Liu¹,
 Jing Yang¹, Ziliang Chen¹, Xiaofei Sun², Keze Wang^{1,†}

¹Sun Yat-sen University

²Alibaba Group

†Corresponding author: kezewang@gmail.com

Abstract

*Multimodal LLMs often produce fluent yet unreliable reasoning, exhibiting weak step-to-step coherence and insufficient visual grounding, largely because existing alignment approaches supervise only the final answer while ignoring the reliability of the intermediate reasoning process. We introduce **SR-MCR**, a lightweight and label-free framework that aligns reasoning by exploiting intrinsic process signals derived directly from model outputs. Five self-referential cues—semantic alignment, lexical fidelity, non-redundancy, visual grounding, and step consistency—are integrated into a normalized, reliability-weighted reward that provides fine-grained process-level guidance. A critic-free GRPO objective, enhanced with a confidence-aware cooling mechanism, further stabilizes training and suppresses trivial or overly confident generations. Built on Qwen2.5-VL, SR-MCR improves both answer accuracy and reasoning coherence across a broad set of visual benchmarks; among open-source models of comparable size, SR-MCR-7B achieves state-of-the-art performance with an average accuracy of 81.4%. Ablation studies confirm the independent contributions of each reward term and the cooling module.*

1. Introduction

Multimodal reasoning must deliver not only correct answers but also explanations that are coherent and visually grounded. Yet recent MLLMs (e.g., LLaVA [32], Qwen-VL [2]) often drift in their intermediate steps—contradicting themselves, hallucinating evidence [28, 43, 62, 70, 73, 79], or repeating trivial content. Existing alignment pipelines, including instruction tuning [50, 61, 71] and preference finetuning (DPO [38, 63], RLHF [36, 44, 72]), rely on costly human-labeled rewards or external evaluators [69, 77]. While effective, they remain brittle under domain shift and largely

outcome-centric, supervising answers rather than the reasoning process [7, 29, 67, 68].

This outcome-centric focus leaves two issues unresolved: (i) *Lack of intrinsic process reward*: supervising only final answers leaves step coherence and visual grounding underconstrained; (ii) *Cross-domain instability*: single reward proxies (e.g., lexical overlap) miscalibrate signals across heterogeneous tasks, causing over-alignment to spurious patterns.

At the same time, a single forward pass of an MLLM already exposes multiple measurable signals that correlate with “good” reasoning—semantic alignment, lexical fidelity, non-redundancy, grounding to visual evidence, and local step consistency [60, 65, 66]. These signals are inexpensive to compute, task-agnostic, and complementary in nature. Rather than relying solely on external preference labels, we ask: *can we turn these process-level signals into a practical, intrinsic self-reward for multimodal reasoning?* We posit that, once normalized and reliability-weighted, such signals can serve as a unified *self-reward* for both training and diagnosis [57, 64, 74].

Based on this observation, we develop **Self-Rewarded Multimodal Coherent Reasoning (SR-MCR)**, a unified framework that instantiates process-aware, label-free alignment for MLLMs. Given an image I , textual input x , and model outputs (\hat{y}_a, \hat{y}_t) (final answer and reasoning trace), SR-MCR computes a normalized self-reward $\mathcal{R}(I, x, \hat{y}_a, \hat{y}_t) = \sum_{k \in \{\text{sem, lex, nr, vis, step}\}} \lambda_k \tilde{s}_k$, $\lambda_k = \frac{\exp(\alpha \text{Relia}_k)}{\sum_j \exp(\alpha \text{Relia}_j)}$. Here $\tilde{s}_k \in [0, 1]$ are min–max normalized scores for semantic similarity, lexical overlap, non-redundancy, visual grounding, and step-wise coherence. The term Relia_k estimates each signal’s reliability (e.g., held-out correlation or inverse variance), producing adaptive weights λ_k that attenuate noisy or unstable signals and amplify consistent ones.

Optimization. Instead of constructing human preference pairs, we directly treat this self-reward as the optimization target and fine-tune the model with a *self-rewarded*

GRPO [42] objective. The policy is updated to increase the likelihood of high-reward generations while constraining drift from the base model via a KL term [14, 40, 41, 55] (Sec. 3, Eq. 9). To further stabilize training under noisy self-rewards, we introduce a dynamic *cooling weight* (Eq. 8) that down-weights trivial or overconfident samples based on their normalized negative log-likelihood [27, 52]. Together, these components yield a simple, label-free, and process-aware alignment recipe that can be applied across diverse visual domains.

Contributions. This work is positioned as a practical, process-centric alignment framework rather than a new RL algorithm. Our main contributions are:

- We identify a key gap in multimodal alignment—the lack of an intrinsic, process-aware reward for coherent and visually grounded reasoning.
- We introduce *SR-MCR*, which fuses five self-signals into a reliability-weighted reward and optimizes MLLMs via GRPO with a simple cooling scheme.
- We provide a lightweight, reproducible recipe that improves accuracy and reasoning coherence over Qwen2.5-VL baselines, with ablations clarifying each component’s role.

2. Related Work

Vision-Language Models. Large Vision-Language Models (VLMs) couple visual encoders (e.g., CLIP [3, 12, 13, 37], ViT [11]) with LLMs for multimodal understanding. CLIP benefits from large-scale contrastive pretraining that yields strong zero-shot transfer and alignment between images and text, but it can struggle with compositional queries, and inherits biases present in its training data. **LLaVA** demonstrated that visual instruction-following can be achieved with a lightweight projector and a two-stage pipeline. Subsequent models such as **Qwen-VL** [75] improved perception and multilinguality via larger data and refined architectures, while **GPT-4V** [35] advanced visual reasoning. **InstructBLIP** [10] further enhances cross-modal fusion through Q-Former [24]. These works establish the foundation of modern multimodal reasoning.

Alignment Methods for VLMs. Early alignment of vision–language models typically begins with **Supervised Fine-Tuning (SFT)** on curated multimodal datasets [25, 26, 31, 49]. While SFT imparts task formats and basic instruction following, it struggles to model nuanced human preferences [9] and often overfits to annotator distributions. **RLHF** extends SFT by training on preference data with a learned reward model [4, 78], improving subjective alignment but incurring substantial annotation cost and introducing potential bias from the reward model itself. In contrast, **RLVR** (Reinforcement Learning with Verifiable Rewards) replaces learned rewards with rule-based or verifier-derived

correctness signals, enabling more transparent and scalable optimization for tasks with objectively checkable outcomes (e.g., VQA or grounded reasoning), and avoiding the failure modes associated with preference-model drift.

Reinforcement Learning Algorithms. **PPO** (Proximal Policy Optimization) is widely used for RL-based alignment; it uses an actor–critic setup with advantage estimation, which is often via GAE, and a clipped surrogate objective to stabilize updates, but requires an additional value (critic) network and thus incurs significant compute and memory overhead. **GRPO** (Group Relative Policy Optimization) [42] removes the critic and constructs relative advantages by comparing rewards within sampled groups of completions, substantially reducing computational and memory cost while retaining strong alignment performance in preference-based generation tasks. In practice, PPO tends to give lower-variance updates at higher resource cost, whereas GRPO is a lightweight alternative that is more sensitive to group construction and reward noise.

3. Method

Following the motivation in Sec. 1, we introduce **Self-Rewarded Multimodal Coherent Reasoning (SR-MCR)**, a training framework that enables multimodal large language models (MLLMs) to *self-evaluate* and *self-improve* their reasoning process without human preference labels [1, 8]. SR-MCR is built on three components: (i) a unified self-reward that aggregates multiple process-level signals, (ii) an adaptive reliability weighting scheme, and (iii) a critic-free GRPO objective with cooling regularization. Together, these components turn multimodal alignment from discrete preference matching into continuous, self-guided optimization over process quality.

3.1. Problem Setup

Given an image I , text input x , a frozen base policy π_0 , and a trainable policy π_θ , the model produces a final answer \hat{y}_a and a reasoning trace \hat{y}_t [22, 51], forming the full response $\hat{y} = (\hat{y}_a, \hat{y}_t)$. Our goal is to align π_θ such that $\hat{y} \sim \pi_\theta(\cdot | I, x)$ is (i) semantically correct, (ii) visually grounded, and (iii) step-wise coherent—*without* human preferences or ground-truth labels. Training relies solely on intrinsic, multi-signal self-rewards derived from (I, x, \hat{y}) .

3.2. Unified Self-Reward

Each forward pass of an MLLM yields several low-cost signals that correlate with reasoning quality. We combine five such signals into a unified, normalized self-reward:

$$R(I, x, \hat{y}_a, \hat{y}_t) = \sum_{k \in \{\text{sem,lex,nr,vis,step}\}} \lambda_k \tilde{s}_k \in [0, 1], \quad (1)$$

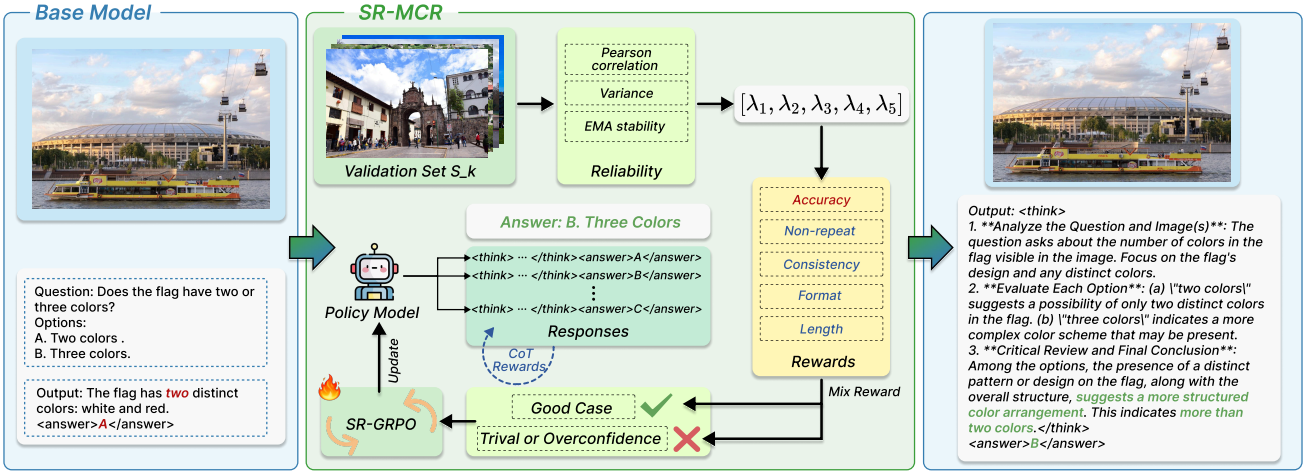


Figure 1. Overview of **SR-MCR**. Given an image–text input (I, x) , the policy π_θ generates multiple responses, each scored by five process-level self-reward terms and an adaptive reliability estimator to form a mixed reward. **SR-GRPO** then favors high-reward, reliable outputs while suppressing trivial ones, updating π_θ on top of the frozen base policy π_0 .

where each raw score s_k is first winsorized (clipped at the 1st and 99th percentiles) and then min–max normalized to $\tilde{s}_k \in [0, 1]$. The five components are: **Semantic consistency** (\tilde{s}_{sem}): sentence-level semantic alignment between reasoning and answer; **Lexical fidelity** (\tilde{s}_{lex}): surface-level overlap between reasoning and answer; **Non-redundancy** (\tilde{s}_{nr}): penalty on repeated n -grams in the reasoning trace; **Visual grounding** (\tilde{s}_{vis}): alignment between textual mentions and visual regions; **Step-wise coherence** (\tilde{s}_{step}): local logical consistency between adjacent steps. All signals are computed purely from the model’s own outputs and pre-trained, frozen tools (e.g., Sentence-BERT [39, 76], CLIP, NER, detection, NLI), and thus do not require ground-truth labels in the training loop.

Semantic and Lexical Signals. We first measure how well the reasoning trace supports the final answer. Let the reasoning trace be split into N sentences $\{\hat{y}_t^{(i)}\}_{i=1}^N$. We define

$$\tilde{s}_{\text{sem}} = \frac{1}{N} \sum_{i=1}^N \cos(f_{\text{SBERT}}(\hat{y}_t^{(i)}), f_{\text{SBERT}}(\hat{y}_a)), \quad (2)$$

where $f_{\text{SBERT}}(\cdot)$ is a Sentence-BERT encoder and $\cos(\cdot, \cdot)$ is cosine similarity. Lexical consistency is quantified via ROUGE-L [30]: $\tilde{s}_{\text{lex}} = \text{ROUGE-L}(\hat{y}_t, \hat{y}_a)$. These signals can optionally be compared against ground-truth answers on a held-out validation set for calibration, but ground truth is *not* required in the training loop.

Non-Redundancy. To discourage degenerate repetition [19], we compute

$$\tilde{s}_{\text{nr}} = 1 - \frac{|\text{repeated } n\text{-grams}(\hat{y}_t)|}{|\text{all } n\text{-grams}(\hat{y}_t)|}, \quad (3)$$

where we use $n = 2$ in our experiments. Higher values correspond to more informative and concise reasoning traces.

Visual Grounding. We align textual mentions in \hat{y}_t with visual regions in I . Textual mentions $\{m_j\}_{j=1}^M$ are extracted using a pretrained NER model (e.g., spaCy). Visual regions $\{r_i\}$ are obtained from a pretrained detector (e.g., DETR [5]) as bounding boxes. We then compute CLIP embeddings and define

$$\tilde{s}_{\text{vis}} = \frac{1}{M} \sum_{j=1}^M \max_i \cos(f_{\text{CLIP}}(r_i), f_{\text{CLIP}}(m_j)), \quad (4)$$

where $f_{\text{CLIP}}(\cdot)$ denotes CLIP encoders for image crops and text spans. AlignScore [59] can be used as a drop-in alternative, but we adopt CLIPScore [18] for efficiency.

Step-wise Coherence. Finally, we assess local logical consistency within the reasoning trace. Let the trace be decomposed into steps $\{\text{step}_1, \dots, \text{step}_L\}$. A pretrained NLI model (e.g., DeBERTa-v3-large [17]) provides entailment probabilities e_i and contradiction probabilities c_i between adjacent steps $(\text{step}_i, \text{step}_{i+1})$. We define

$$\tilde{s}_{\text{step}} = \frac{1}{L-1} \sum_{i=1}^{L-1} \min(e_i, 1 - c_i), \quad (5)$$

which encourages both strong entailment and low contradiction between consecutive steps.

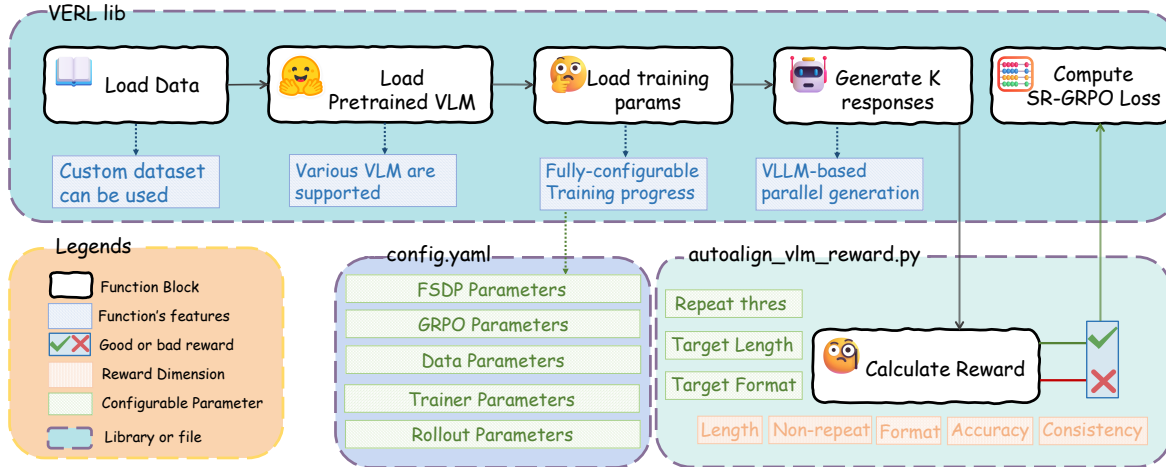


Figure 2. Training pipeline of SR-MCR. We load data and a pretrained VLM, sample K responses via vLLM [23], compute component-wise self-rewards, and train a LoRA adapter with the SR-GRPO loss. Rewards and hyperparameters are specified in a single YAML configuration.

Adaptive Reliability Weighting. Different signals may have varying reliability across domains (e.g., lexical overlap is more informative in QA than in math reasoning). We therefore assign adaptive weights λ_k based on a reliability score Relia_k :

$$\lambda_k = \frac{\exp(\alpha \text{Relia}_k)}{\sum_j \exp(\alpha \text{Relia}_j)}, \quad \sum_k \lambda_k = 1, \quad (6)$$

where $\alpha > 0$ is a temperature that controls sharpness. The reliability score Relia_k can be instantiated as

$$\text{Relia}_k \in \{\rho_k, 1/\text{Var}[s_k], \text{EMA-stability}(s_k)\}. \quad (7)$$

Here ρ_k denotes the Pearson correlation between the raw score s_k and task accuracy on a small, labeled validation set (optional). This calibration stage is the *only* place that may use ground-truth labels; the main optimization in Sec. 3.3 is fully self-rewarded. If no labeled validation set exists, we use GT-free proxies—inverse variance, EMA stability, or uniform weights $\lambda_k = 1/5$.

3.3. Self-Rewarded GRPO with Cooling

To optimize continuous self-rewards without constructing preference pairs, we adopt the **Generalized Reversed Policy Optimization (GRPO)** objective. Directly using the normalized self-reward R in Eq. (1) can be unstable, as low-reward trivial samples and overconfident degenerate ones introduce noisy gradients. We therefore define an *adjusted reward* that applies reward- and confidence-aware cooling:

$$R_{\text{adj}}(\hat{y}) = \tilde{R}(\hat{y})^\gamma \cdot \sigma(\kappa(\bar{\ell}_\theta(\hat{y}) - c)), \quad (8)$$

where $\tilde{R}(\hat{y}) \in [0, 1]$ is the (optionally re-normalized) self-reward, $\bar{\ell}_\theta(\hat{y})$ is the average token negative log-likelihood

Algorithm 1 SR-MCR: Self-Rewarded GRPO Training Loop

- 1: **Input:** base policy π_0 , trainable policy π_θ
- 2: **Hyperparameters:** learning rate η , KL weight β_{KL}
- 3: **for** each training iteration **do**
- 4: **Candidate sampling:** sample K responses $\mathcal{C} \leftarrow \{\hat{y}^{(i)} \sim \pi_\theta(\cdot | I, x)\}_{i=1}^K$
- 5: **Reward computation:** compute $\{s_k\}$ and fuse into R via Eq. (1)
- 6: **Reliability update:** update Relia_k (e.g., EMA or variance), then λ_k via Eq. (6)
- 7: **Policy update:** compute $R_{\text{adj}}(\hat{y})$ via Eq. (8) and $\mathcal{L}_{\text{SR-GRPO}}$ via Eq. (9)
- 8: update parameters $\theta \leftarrow \theta - \eta \nabla_\theta \mathcal{L}_{\text{SR-GRPO}}$
- 9: **Monitoring:** track component rewards and coherence violations; early-stop when a moving average of R plateaus
- 10: **end for**
- 11: **Return:** optimized policy π_θ

(NLL) under π_θ , $\sigma(\cdot)$ is the sigmoid function, and γ , κ , c are hyperparameters controlling reward scaling, cooling sharpness, and the NLL baseline (e.g., $\gamma = 1.0$, $\kappa = 5.0$, $c = 0.1$).

This design downweights gradients from two types of uninformative samples: (i) *trivial low-reward* samples, where $\tilde{R}(\hat{y}) \rightarrow 0$ drives $R_{\text{adj}}(\hat{y}) \rightarrow 0$, and (ii) *overconfident* samples, where $\bar{\ell}_\theta(\hat{y}) < c$ makes the sigmoid term close to zero. By contrast, high-reward yet moderately uncertain samples obtain the strongest gradient signal.

Table 1. **Multimodal benchmark results.** SR-MCR (3B/7B) improves its Qwen2.5-VL bases and is competitive with prior models. Best open-source results in **bold**. *Models with a separate “Thinking” mode.

Model	MMMU _{val}	MMB _{v1.1}	MME	ChartQA _{test}	AI2D	HallBench	Avg.
<i>Closed-source Models</i>							
Gemini-2.0-Pro	72.6	83.0	86.1	91.2	84.8	49.8	77.9
GPT-4o-latest	70.7	84.3	84.2	91.5	86.3	57.0	79.0
<i>Open-source Models (Baselines)</i>							
InternVL3-2B	47.1	84.3	77.4	80.4	78.7	41.4	68.2
Qwen2.5-VL-3B	48.1	82.4	77.5	87.0	80.7	48.3	70.7
WeThink-7B	50.9	87.8	82.9	90.8	84.5	55.1	75.3
InternVL3-8B	57.3	87.7	85.2	89.6	85.2	53.7	76.5
Qwen2.5-VL-7B	50.3	86.7	82.2	89.5	84.0	56.0	74.8
VL-Rethinker-7B	54.8	88.2	82.9	91.5	83.6	55.1	76.0
VLAA-Thinker-7B	51.9	86.9	83.3	89.5	78.9	51.5	73.7
Keye-VL-8B-Thinking*	63.4	81.7	83.5	88.0	86.4	62.7	77.6
Kimi-VL-A3B-Thinking*	60.4	89.7	87.0	92.1	83.1	58.3	78.4
SAIL-VL2-8B-Thinking*	66.1	90.4	86.0	93.6	87.4	61.5	80.8
<i>Our Models (SR-MCR)</i>							
SR-MCR-3B	52.8	86.9	80.8	90.9	84.3	51.9	74.6
SR-MCR-7B	67.6	91.2	87.3	94.5	88.2	59.4	81.4

We finally optimize the model with the SR-GRPO loss:

$$\mathcal{L}_{\text{SR-GRPO}} = -\mathbb{E}_{(I, x), \hat{y} \sim \pi_\theta} \left[R_{\text{adj}}(\hat{y}) \log \frac{\pi_\theta(\hat{y} | I, x)}{\pi_0(\hat{y} | I, x)} \right] + \beta_{\text{KL}} \text{KL}(\pi_\theta \| \pi_0). \quad (9)$$

Interpretation and Pipeline. The first term steers π_θ toward responses it deems coherent and grounded, while the KL term limits drift from π_0 . Unlike pairwise objectives (e.g., DPO, RLHF), SR-GRPO optimizes continuous self-rewards, yielding smoother and more stable label-free training. We train a LoRA adapter [20] on the frozen backbone and re-rank M sampled candidates using R at inference. Without reference answers, SR-MCR falls back to (vis, nr, step), which still enforces visual grounding and step coherence.

4. Experiments

4.1. Experimental Setup

Backbone and Training. We adopt Qwen2.5-VL [48] as the base multimodal backbone. We then apply our proposed **Self-Rewarded Multimodal Coherent Reasoning (SR-MCR)** training procedure, which leverages GRPO with step-wise reasoning coherence rewards. All training is performed efficiently using LoRA on top of the original checkpoints. Crucially, our method does not require training any external reward model and produces a **sin-**

gle, unified model, obviating the need for separate “Instruct” vs. “Thinking” variants common in prior work.

Benchmarks. We evaluate our models on a comprehensive suite of benchmarks. For general multimodal understanding (evaluated using **ACC**, results in Table 1), we use: **MMMU_{val}** [58] — general-domain knowledge and reasoning across diverse subjects; **MMBench_{v1.1}** [33] — instruction-following, world knowledge, and general perception; **MME** [15] — fine-grained vision–language alignment and grounding; **ChartQA_{test}** [34] — table and chart understanding with numerical reasoning; **AI2D** [21] — diagram parsing and diagrammatic reasoning; **HallBench** [16] — robustness against visual and factual hallucination. Additionally, we specifically evaluate comprehensive visual reasoning using **V*Bench** [53] (results in Table 2).

4.2. Main Results on General Benchmarks

Key Finding. As shown in Table 1, **SR-MCR-7B** achieves the best average score (**81.4**) among open-source VLMs and surpasses other “Thinking” variants *without* requiring their dual-checkpoint (Instruct/Thinking) setup.

Scalability and Efficacy. SR-MCR delivers consistent gains over its Qwen2.5-VL bases at both 3B (**74.6** vs. 70.7, +3.9) and 7B (**81.4** vs. 74.8, +6.6). This shows that our *reasoning-coherence alignment* effectively scales across model sizes, rather than relying on size-driven improvements.

Table 2. **Evaluation on V* Bench.** SR-MCR compared with Qwen2.5-VL and other VLMs. Best open-source results in **bold**.
 *Models with a “Thinking” mode.

Model	Attribute	Spatial	Overall
<i>Closed-source Models</i>			
GPT-4o	62.03	72.00	66.00
<i>Open-source Models</i>			
InternVL3-2B [80]	59.13	63.16	60.73
Qwen2.5-VL-3B	78.26	60.53	71.20
VLAA-Thinker-7B [6]	56.52	59.21	57.59
WeThink-7B [54]	82.61	75.00	79.58
VL-Rethinker-7B [47]	64.35	71.05	67.02
InternVL3-8B	70.43	72.37	71.20
Keye-VL-8B- Thinking [46]*	66.96	75.00	70.16
Qwen2.5-VL-7B	80.87	75.00	78.53
Kimi-VL-A3B- Thinking* [45]	51.30	60.53	54.97
SAIL-VL2-8B- Thinking [56]*	51.30	65.79	57.07
<i>Our Models (SR-MCR)</i>			
SR-MCR-3B (Ours)	81.16	61.60	73.12
SR-MCR-7B (Ours)	83.48	76.32	80.63

4.3. Results on V* Bench

Performance on V* Bench. As shown in Table 2, our SR-MCR models continue to demonstrate strong performance on this challenging benchmark focused on spatial and attribute understanding. The **SR-MCR-7B** model achieves state-of-the-art results among all open-source models on the **Overall** score (**80.63**) and the **Attribute** sub-benchmark (**83.48**). It also secures the top open-source score for **Spatial** reasoning (**76.32**). This further validates that our SR-MCR training procedure effectively enhances complex, fine-grained reasoning capabilities.

4.4. Analysis

To evaluate the effectiveness of SR-MCR, we conduct ablations on both 3B and 7B models and report the **Avg.** performance across general benchmarks (Table 1).

4.5. MME Accuracy on Various Steps

As shown in Fig. 3, MME ACC+ steadily increases with training steps across the four task types, indicating a consistent strengthening of multimodal reasoning. Code reasoning and numerical calculation exhibit the fastest early-stage gains, suggesting that the model quickly absorbs structural and arithmetic patterns. OCR begins with a higher baseline and therefore improves only slightly. Commonsense reasoning grows more slowly, reflecting its relatively greater complexity.

Table 3. **Ablation on Reward Components.** Comparison of full SR-MCR and variants dropping each reward term, using average scores from Table 1 for 3B and 7B.

Configuration	3B Scale	7B Scale
<i>Full Method</i>		
SR-MCR (Full Method)	74.6	81.4
<i>— Remove one component —</i>		
w/o \tilde{s}_{sem} (semantic)	73.9	80.5
w/o \tilde{s}_{lex} (lexical)	74.1	80.9
w/o \tilde{s}_{nr} (non-redundant)	73.5	80.2
w/o \tilde{s}_{vis} (visual)	72.0	78.5
w/o \tilde{s}_{step} (coherence)	71.8	78.1
<i>— Use key components only —</i>		
Only $\tilde{s}_{\text{vis}} + \tilde{s}_{\text{step}}$	74.0	80.7
<i>Base Model</i>		
Base Model (Qwen2.5-VL)	70.7	74.8

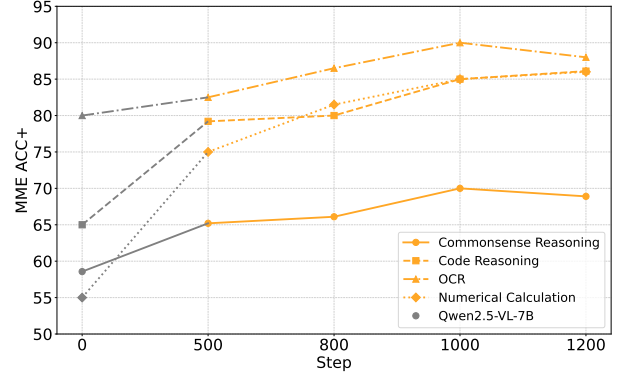


Figure 3. MME ACC+ performance at different training steps across four task types. ACC+ is counted only when both QA pairs for an image are correctly answered.

After around 1k steps, most tasks begin to plateau. OCR even shows a minor dip, which may indicate mild overfitting or a trade-off introduced during optimization. Overall, the trends suggest that most improvements occur early, with later steps offering diminishing returns.

Ablation on Reward Components

Experimental Setup. We study the unified five-component self-reward \mathcal{R} (Section 3.2) by removing each term individually on both model scales. We also test a two-term variant using only \tilde{s}_{vis} (visual grounding) and \tilde{s}_{step} (step-wise coherence).

Results and Analysis. Table 3 shows that:

(1) All components matter. Removing any reward term consistently reduces performance on both 3B and 7B mod-

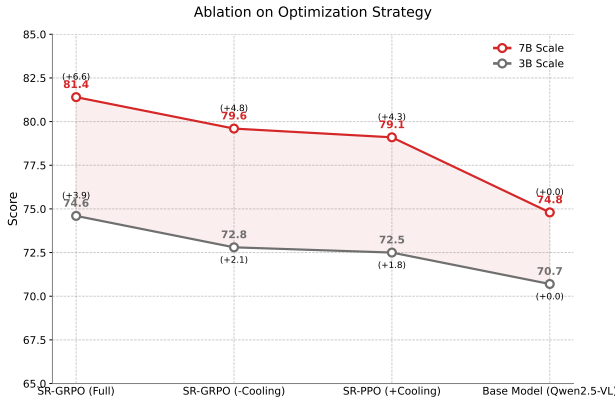


Figure 4. **Ablation on Optimization Strategy.** SR-GRPO (cooling) vs. PPO and no-cooling. Avg. 3B/7B scores show both GRPO and cooling are needed.

els.

(2) Grounding and coherence are critical. The largest drops occur when ablating \tilde{s}_{vis} or \tilde{s}_{step} , confirming their central role in visual-semantic alignment and reasoning stability.

(3) Unified reward is optimal. While $\tilde{s}_{vis} + \tilde{s}_{step}$ performs well (80.7 on 7B), the full five-term reward yields the best results (81.4), showing that auxiliary terms (\tilde{s}_{sem} , \tilde{s}_{lex} , \tilde{s}_{nr}) provide complementary constraints.

Ablation on Optimization Strategy

Experimental Setup. We compare our full method with two variants: (a) SR-GRPO without cooling ($R_{adj} = \bar{R}$), and (b) SR-PPO, which replaces GRPO with PPO and trains a separate critic.

Results and Analysis. Figure 4 shows two main findings. **(1) Cooling is essential.** Removing the cooling module leads to consistent drops (3B: 74.6 → 72.8; 7B: 81.4 → 79.6), indicating that R_{adj} stabilizes training by down-weighting trivial or overly confident samples.

(2) GRPO outperforms PPO. SR-GRPO (81.4 on 7B) surpasses SR-PPO (79.1), suggesting that the critic-free GRPO formulation better fits continuous self-reward signals and avoids instability from value estimation.

4.6. Analysis of Reasoning Process Quality

We evaluated whether SR-MCR improves not only final answer accuracy but also the quality of underlying reasoning. We extracted full chains of thought from Qwen2.5-VL-7B and SR-MCR-7B, then conducted a randomized, blind A/B study on 100 independently sampled cases. GPT-4o (2024-11-20) judged each pair on coherence, logical soundness, and completeness. SR-MCR-7B was preferred in 90.82% of evaluations, versus 9.18% for Qwen2.5-VL-7B. As summarized in Fig. 5, these results indicate that SR-MCR significantly enhances the clarity, correctness, and complete-

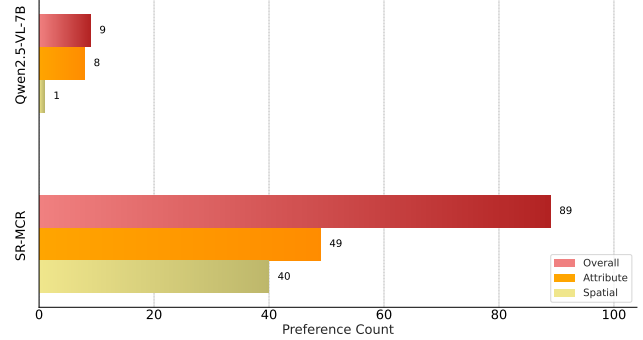


Figure 5. Reasoning quality evaluation. On 100 A/B samples, SR-MCR-7B is preferred (90.82%) over the Qwen2.5-VL-7B baseline (9.18%).

ness of reasoning, supporting more reliable downstream answers.

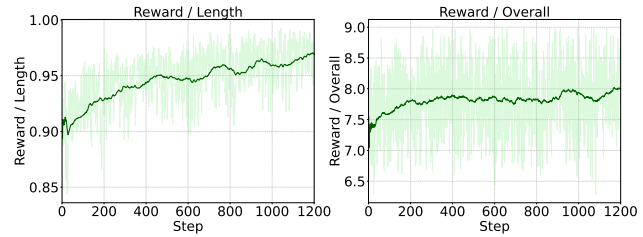


Figure 6. Reward curves for SR-MCR-7B. Both Length and Overall Rewards increase steadily, indicating improved reasoning.

4.7. Analysis of Training Progress

To examine how reasoning ability evolves during training, we analyze the reward curve of SR-MCR-7B in Fig. 6. The Length Reward rises sharply, indicating that SR-MCR encourages longer and more articulated reasoning chains. Meanwhile, the overall reward increases simultaneously, showing that these extended trajectories correspond to genuine improvements in reasoning quality rather than simple verbosity. The joint rise of both signals suggests that the model learns to produce longer explanations only when they contribute meaningful structure and clarity. Overall, this pattern reflects that SR-MCR gradually strengthens the model’s ability to generate complete, coherent reasoning processes, leading to steady gains on complex tasks.

5. Conclusion

We introduced **SR-MCR**, which fuses five intrinsic self-signals into a reliability-weighted reward and aligns multimodal reasoning through cooling-stabilized GRPO. It improves accuracy, grounding, and coherence over Qwen2.5-VL. Future work includes video reasoning, uncertainty modeling, and larger-scale pretraining.

References

- [1] Akari Asai, Zeqiu Wu, Yizhong Wang, Avirup Sil, and Hannaneh Hajishirzi. Self-RAG: Learning to retrieve, generate, and critique through self-reflection. *arXiv preprint arXiv:2310.11511*, 2023. 2
- [2] Jinze Bai, Shuai Bai, Shusheng Yang, Shijie Wang, Sinan Tan, Peng Wang, Junyang Lin, Chang Zhou, and Jingren Zhou. Qwen-vl: A versatile vision-language model for understanding, localization, text reading, and beyond. *arXiv preprint arXiv:2308.12966*, 2023. 1
- [3] Kaitong Cai, Jusheng Zhang, Yijia Fan, Jing Yang, and Keze Wang. Racot: Plug-and-play contrastive example generation mechanism for enhanced llm reasoning reliability, 2025. arXiv:2510.22710. 2
- [4] Kaitong Cai, Jusheng Zhang, Jing Yang, Yijia Fan, Pengtao Xie, Jian Wang, and Keze Wang. Flashvlm: Text-guided visual token selection for large multimodal models, 2025. arXiv:2512.20561. 2
- [5] Nicolas Carion, Francisco Massa, Gabriel Synnaeve, Nicolas Usunier, Alexander Kirillov, and Sergey Zagoruyko. End-to-end object detection with transformers. *CoRR*, abs/2005.12872, 2020. 3
- [6] Hardy Chen, Haoqin Tu, Fali Wang, Hui Liu, Xianfeng Tang, Xinya Du, Yuyin Zhou, and Cihang Xie. Sft or rl? an early investigation into training rl-like reasoning large vision-language models, 2025. 6
- [7] Yangyi Chen, Karan Sikka, Michael Cogswell, Heng Ji, and Ajay Divakaran. Measuring and improving chain-of-thought reasoning in vision-language models. Mexico City, Mexico, 2024. Association for Computational Linguistics. 1
- [8] Zixiang Chen, Yihe Deng, Huizhuo Yuan, Kaixuan Ji, and Quanquan Gu. Self-play fine-tuning convertsweak language models to strong language models. In *Proceedings of the 41st International Conference on Machine Learning*. JMLR.org, 2024. 2
- [9] Paul F. Christiano, Jan Leike, Tom B. Brown, Miljan Martic, Shane Legg, and Dario Amodei. Deep reinforcement learning from human preferences. In *Proceedings of the 31st International Conference on Neural Information Processing Systems*, page 4302–4310, Red Hook, NY, USA, 2017. Curran Associates Inc. 2
- [10] Wenliang Dai, Junnan Li, Dongxu Li, Anthony Meng Huat Tiong, Junqi Zhao, Weisheng Wang, Boyang Li, Pascale Fung, and Steven Hoi. Instructblip: towards general-purpose vision-language models with instruction tuning. In *Proceedings of the 37th International Conference on Neural Information Processing Systems*, Red Hook, NY, USA, 2023. Curran Associates Inc. 2
- [11] Alexey Dosovitskiy, Lucas Beyer, Alexander Kolesnikov, Dirk Weissenborn, Xiaohua Zhai, Thomas Unterthiner, Mostafa Dehghani, Matthias Minderer, Georg Heigold, Sylvain Gelly, Jakob Uszkoreit, and Neil Houlsby. An image is worth 16x16 words: Transformers for image recognition at scale. In *9th International Conference on Learning Representations, ICLR 2021, Virtual Event, Austria, May 3-7, 2021*. OpenReview.net, 2021. 2
- [12] Yijia Fan, Jusheng Zhang, Kaitong Cai, Jing Yang, Chengpei Tang, Jian Wang, and Keze Wang. Cost-effective communication: An auction-based method for language agent interaction, 2025. arXiv:2511.13193. 2
- [13] Yijia Fan, Jusheng Zhang, Kaitong Cai, Jing Yang, Jian Wang, and Keze Wang. 3dalign-daer: Dynamic attention policy and efficient retrieval strategy for fine-grained 3d-text alignment at scale, 2025. arXiv:2511.13211. 2
- [14] Yijia Fan, Jusheng Zhang, Kaitong Cai, Jing Yang, and Keze Wang. CCG: Rare-label prediction via neural SEM–driven causal game. In *Findings of the Association for Computational Linguistics: EMNLP 2025*, pages 6243–6256, Suzhou, China, 2025. Association for Computational Linguistics. 2
- [15] Chaoyou Fu, Peixian Chen, Yunhang Shen, Yulei Qin, Mengdan Zhang, Xu Lin, Jinrui Yang, Xiawu Zheng, Ke Li, Xing Sun, Yunsheng Wu, Rongrong Ji, Caifeng Shan, and Ran He. Mme: A comprehensive evaluation benchmark for multimodal large language models, 2025. 5
- [16] Tianrui Guan, Fuxiao Liu, Xiyang Wu, Ruiqi Xian, Zongxia Li, Xiaoyu Liu, Xijun Wang, Lichang Chen, Furong Huang, Yaser Yacoob, Dinesh Manocha, and Tianyi Zhou. Hallucinationbench: An advanced diagnostic suite for entangled language hallucination and visual illusion in large vision-language models. In *Proceedings of the IEEE/CVF Conference on Computer Vision and Pattern Recognition (CVPR)*, pages 14375–14385, 2024. 5
- [17] Pengcheng He, Xiaodong Liu, Jianfeng Gao, and Weizhu Chen. Deberta: Decoding-enhanced BERT with disentangled attention. *CoRR*, abs/2006.03654, 2020. 3
- [18] Jack Hessel, Ari Holtzman, Maxwell Forbes, Ronan Le Bras, and Yejin Choi. CLIPScore: a reference-free evaluation metric for image captioning. In *EMNLP*, 2021. 3
- [19] Ari Holtzman, Jan Buys, Maxwell Forbes, and Yejin Choi. The curious case of neural text degeneration. *CoRR*, abs/1904.09751, 2019. 3
- [20] Edward J. Hu, Yelong Shen, Phillip Wallis, Zeyuan Allen-Zhu, Yuanzhi Li, Shean Wang, and Weizhu Chen. Lora: Low-rank adaptation of large language models. *CoRR*, abs/2106.09685, 2021. 5
- [21] Aniruddha Kembhavi, Mike Salvato, Eric Kolve, Min Joon Seo, Hannaneh Hajishirzi, and Ali Farhadi. A diagram is worth A dozen images. *CoRR*, abs/1603.07396, 2016. 5
- [22] Takeshi Kojima, Shixiang Shane Gu, Machel Reid, Yutaka Matsuo, and Yusuke Iwasawa. Large language models are zero-shot reasoners. In *Proceedings of the 36th International Conference on Neural Information Processing Systems*, Red Hook, NY, USA, 2022. Curran Associates Inc. 2
- [23] Woosuk Kwon, Zhuohan Li, Siyuan Zhuang, Ying Sheng, Lianmin Zheng, Cody Hao Yu, Joseph E. Gonzalez, Hao Zhang, and Ion Stoica. Efficient memory management for large language model serving with pagedattention. In *Proceedings of the ACM SIGOPS 29th Symposium on Operating Systems Principles*, 2023. 4
- [24] Junnan Li, Dongxu Li, Silvio Savarese, and Steven Hoi. Blip-2: bootstrapping language-image pre-training with frozen image encoders and large language models. In *Proceedings of the 40th International Conference on Machine Learning*. JMLR.org, 2023. 2

[25] Lei Li, Yuwei Yin, Shicheng Li, Liang Chen, Peiyi Wang, Shuhuai Ren, Mukai Li, Yazheng Yang, Jingjing Xu, Xu Sun, Lingpeng Kong, and Qi Liu. M³it: A large-scale dataset towards multi-modal multilingual instruction tuning. *arXiv preprint arXiv:2306.04387*, 2023. 2

[26] Xiaohua Li, Jusheng Zhang, and Fatemeh Safara. Improving the accuracy of diabetes diagnosis applications through a hybrid feature selection algorithm. *Neural Process. Lett.*, 55(1):153–169, 2021. 2

[27] Xiang Lisa Li, Ari Holtzman, Daniel Fried, Percy Liang, Jason Eisner, Tatsunori Hashimoto, Luke Zettlemoyer, and Mike Lewis. Contrastive decoding: Open-ended text generation as optimization. pages 12286–12312, Toronto, Canada, 2023. Association for Computational Linguistics. 2

[28] Yifan Li, Yifan Du, Kun Zhou, Jinpeng Wang, Xin Zhao, and Ji-Rong Wen. Evaluating object hallucination in large vision-language models. In *Proceedings of the 2023 Conference on Empirical Methods in Natural Language Processing*, pages 292–305, Singapore, 2023. Association for Computational Linguistics. 1

[29] Hunter Lightman, Vineet Kosaraju, Yura Burda, Harri Edwards, Bowen Baker, Teddy Lee, Jan Leike, John Schulman, Ilya Sutskever, and Karl Cobbe. Let’s verify step by step, 2023. 1

[30] Chin-Yew Lin. ROUGE: A package for automatic evaluation of summaries. In *Text Summarization Branches Out*, pages 74–81, Barcelona, Spain, 2004. Association for Computational Linguistics. 3

[31] Wenjun Lin, Jensen Zhang, Kaitong Cai, and Keze Wang. Storm: Search-guided generative world models for robotic manipulation, 2025. 2

[32] Haotian Liu, Chunyuan Li, Qingyang Wu, and Yong Jae Lee. Visual instruction tuning, 2023. 1

[33] Yuan Liu, Haodong Duan, Yuanhan Zhang, Bo Li, Songyang Zhang, Wangbo Zhao, Yike Yuan, Jiaqi Wang, Conghui He, Ziwei Liu, et al. Mmbench: Is your multi-modal model an all-around player? In *European conference on computer vision*, pages 216–233. Springer, 2024. 5

[34] Ahmed Masry, Do Xuan Long, Jia Qing Tan, Shafiq Joty, and Enamul Hoque. ChartQA: A benchmark for question answering about charts with visual and logical reasoning. In *Findings of the Association for Computational Linguistics: ACL 2022*, pages 2263–2279, Dublin, Ireland, 2022. Association for Computational Linguistics. 5

[35] OpenAI. GPT-4V(ision). <https://openai.com/contributions/gpt-4v/>, 2023. 2

[36] Long Ouyang, Jeff Wu, Xu Jiang, Diogo Almeida, Carroll L. Wainwright, Pamela Mishkin, Chong Zhang, Sandhini Agarwal, Katarina Slama, Alex Ray, John Schulman, Jacob Hilton, Fraser Kelton, Luke Miller, Maddie Simens, Amanda Askell, Peter Welinder, Paul Christiano, Jan Leike, and Ryan Lowe. Training language models to follow instructions with human feedback. In *Proceedings of the 36th International Conference on Neural Information Processing Systems*, Red Hook, NY, USA, 2022. Curran Associates Inc. 1

[37] Alec Radford, Jong Wook Kim, Chris Hallacy, Aditya Ramesh, Gabriel Goh, Sandhini Agarwal, Girish Sastry, Amanda Askell, Pamela Mishkin, Jack Clark, Gretchen Krueger, and Ilya Sutskever. Learning transferable visual models from natural language supervision. *CoRR*, abs/2103.00020, 2021. 2

[38] Rafael Raffailov, Archit Sharma, Eric Mitchell, Stefano Ermon, Christopher D. Manning, and Chelsea Finn. Direct preference optimization: your language model is secretly a reward model. In *Proceedings of the 37th International Conference on Neural Information Processing Systems*, Red Hook, NY, USA, 2023. Curran Associates Inc. 1

[39] Nils Reimers and Iryna Gurevych. Sentence-bert: Sentence embeddings using siamese bert-networks. *CoRR*, abs/1908.10084, 2019. 3

[40] John Schulman, Sergey Levine, Philipp Moritz, Michael I. Jordan, and Pieter Abbeel. Trust region policy optimization. *CoRR*, abs/1502.05477, 2015. 2

[41] John Schulman, Filip Wolski, Prafulla Dhariwal, Alec Radford, and Oleg Klimov. Proximal policy optimization algorithms. *CoRR*, abs/1707.06347, 2017. 2

[42] Zhihong Shao, Peiyi Wang, Qihao Zhu, Runxin Xu, Junxiao Song, Mingchuan Zhang, Y. K. Li, Y. Wu, and Daya Guo. Deepseekmath: Pushing the limits of mathematical reasoning in open language models, 2024. 2

[43] Aviv Slobodkin, Omer Goldman, Avi Caciularu, Ido Dagan, and Shauli Ravfogel. The curious case of hallucinatory (un)answerability: Finding truths in the hidden states of over-confident large language models. In *Proceedings of the 2023 Conference on Empirical Methods in Natural Language Processing*, pages 3607–3625, Singapore, 2023. Association for Computational Linguistics. 1

[44] Nisan Stiennon, Long Ouyang, Jeff Wu, Daniel M. Ziegler, Ryan Lowe, Chelsea Voss, Alec Radford, Dario Amodei, and Paul Christiano. Learning to summarize from human feedback. In *Proceedings of the 34th International Conference on Neural Information Processing Systems*, Red Hook, NY, USA, 2020. Curran Associates Inc. 1

[45] Kimi Team, Angang Du, Bohong Yin, Bowei Xing, Bowen Qu, Bowen Wang, Cheng Chen, Chenlin Zhang, Chenzhuang Du, Chu Wei, Congcong Wang, Dehao Zhang, Dikang Du, Dongliang Wang, Enming Yuan, Enzhe Lu, Fang Li, Flood Sung, Guangda Wei, Guokun Lai, Han Zhu, Hao Ding, Hao Hu, Hao Yang, Hao Zhang, Haoning Wu, Haotian Yao, Haoyu Lu, Heng Wang, Hongcheng Gao, Huabin Zheng, Jiaming Li, Jianlin Su, Jianzhou Wang, Jiaqi Deng, Jiezhong Qiu, Jin Xie, Jinhong Wang, Jingyuan Liu, Junjie Yan, Kun Ouyang, Liang Chen, Lin Sui, Longhui Yu, Mengfan Dong, Mengnan Dong, Nuo Xu, Pengyu Cheng, Qizheng Gu, Runjie Zhou, Shaowei Liu, Sihan Cao, Tao Yu, Tianhui Song, Tongtong Bai, Wei Song, Weiran He, Weixiao Huang, Weixin Xu, Xiaokun Yuan, Xingcheng Yao, Xingzhe Wu, Xinxing Zu, Xinyu Zhou, Xinyuan Wang, Y. Charles, Yan Zhong, Yang Li, Yangyang Hu, Yanru Chen, Yejie Wang, Yibo Liu, Yibo Miao, Yidao Qin, Yimin Chen, Yiping Bao, Yiqin Wang, Yongsheng Kang, Yuanxin Liu, Yulun Du, Yuxin Wu, Yuzhi Wang, Yuzi Yan, Zaida Zhou, Zhaowei Li, Zhejun Jiang, Zheng Zhang, Zhilin Yang, Zhiqi Huang, Zihao Huang, Zijia Zhao, and Ziwei Chen. Kimi-VL technical report, 2025. 6

[46] Kwai Keye Team. Kwai keye-vl technical report, 2025. 6

[47] Haozhe Wang, Chao Qu, Zuming Huang, Wei Chu, Fangzhen Lin, and Wenhui Chen. Vl-rethinker: Incentivizing self-reflection of vision-language models with reinforcement learning. *arXiv preprint arXiv:2504.08837*, 2025. 6

[48] Peng Wang, Shuai Bai, Sinan Tan, Shijie Wang, Zhihao Fan, Jinze Bai, Keqin Chen, Xuejing Liu, Jialin Wang, Wenbin Ge, Yang Fan, Kai Dang, Mengfei Du, Xuancheng Ren, Rui Men, Dayiheng Liu, Chang Zhou, Jingren Zhou, and Junyang Lin. Qwen2-vl: Enhancing vision-language model's perception of the world at any resolution, 2024. 5

[49] Yizhong Wang, Yeganeh Kordi, Swaroop Mishra, Alisa Liu, Noah A. Smith, Daniel Khashabi, and Hannaneh Hajishirzi. Self-instruct: Aligning language model with self generated instructions, 2022. 2

[50] Jason Wei, Maarten Bosma, Vincent Y. Zhao, Kelvin Guu, Adams Wei Yu, Brian Lester, Nan Du, Andrew M. Dai, and Quoc V. Le. Finetuned language models are zero-shot learners. In *The Tenth International Conference on Learning Representations, ICLR 2022, Virtual Event, April 25-29, 2022*. OpenReview.net, 2022. 1

[51] Jason Wei, Xuezhi Wang, Dale Schuurmans, Maarten Bosma, Brian Ichter, Fei Xia, Ed H. Chi, Quoc V. Le, and Denny Zhou. Chain-of-thought prompting elicits reasoning in large language models. In *Proceedings of the 36th International Conference on Neural Information Processing Systems*, Red Hook, NY, USA, 2022. Curran Associates Inc. 2

[52] Sean Welleck, Ilia Kulikov, Stephen Roller, Emily Dinan, Kyunghyun Cho, and Jason Weston. Neural text generation with unlikelihood training. *CoRR*, abs/1908.04319, 2019. 2

[53] Penghao Wu and Saining Xie. V*: Guided visual search as a core mechanism in multimodal llms. *arXiv preprint arXiv:2312.14135*, 2023. 5

[54] Jie Yang, Feipeng Ma, Zitian Wang, Dacheng Yin, Kang Rong, Fengyun Rao, and Ruimao Zhang. Wethink: Toward general-purpose vision-language reasoning via reinforcement learning, 2025. 6

[55] Jiawei Yao, Jusheng Zhang, Xiaochao Pan, Tong Wu, and Canran Xiao. Depthssc: Monocular 3d semantic scene completion via depth-spatial alignment and voxel adaptation, 2024. 2

[56] Weijie Yin, Yongjie Ye, Fangxun Shu, Yue Liao, Zijian Kang, Hongyuan Dong, Haiyang Yu, Dingkang Yang, Jiacong Wang, Han Wang, Wenzhuo Liu, Xiao Liang, Shuicheng Yan, and Chao Feng. Sail-vl2 technical report, 2025. 6

[57] Weizhe Yuan, Richard Yuanzhe Pang, Kyunghyun Cho, Sainbayar Sukhbaatar, Jing Xu, and Jason Weston. Self-rewarding language models, 2024. 1

[58] Xiang Yue, Yuansheng Ni, Kai Zhang, Tianyu Zheng, Ruoji Liu, Ge Zhang, Samuel Stevens, Dongfu Jiang, Weiming Ren, Yuxuan Sun, Cong Wei, Botao Yu, Ruibin Yuan, Renliang Sun, Ming Yin, Boyuan Zheng, Zhenzhu Yang, Yibo Liu, Wenhao Huang, Huan Sun, Yu Su, and Wenhui Chen. Mmmu: A massive multi-discipline multimodal understanding and reasoning benchmark for expert agi. In *Proceedings of CVPR*, 2024. 5

[59] Yuheng Zha, Yichi Yang, Ruichen Li, and Zhitong Hu. Align-Score: Evaluating factual consistency with a unified alignment function. In *Proceedings of the 61st Annual Meeting of the Association for Computational Linguistics (Volume 1: Long Papers)*, pages 11328–11348, Toronto, Canada, 2023. Association for Computational Linguistics. 3

[60] Hanning Zhang, Shizhe Diao, Yong Lin, Yi Fung, Qing Lian, Xingyao Wang, Yangyi Chen, Heng Ji, and Tong Zhang. R-tuning: Instructing large language models to say 'I don't know'. pages 7113–7139, Mexico City, Mexico, 2024. Association for Computational Linguistics. 1

[61] Jusheng Zhang, Kaitong Cai, Yijia Fan, Ningyuan Liu, and Keze Wang. MAT-agent: Adaptive multi-agent training optimization. In *The Thirty-ninth Annual Conference on Neural Information Processing Systems*, 2025. 1

[62] Jusheng Zhang, Kaitong Cai, Yijia Fan, Jian Wang, and Keze Wang. CF-VLM: Counterfactual vision-language fine-tuning. In *Advances in Neural Information Processing Systems*, 2025. OpenReview: <https://openreview.net/forum?id=0qGtaRTsCo>. 1

[63] Jusheng Zhang, Kaitong Cai, Xiaoyang Guo, Sidi Liu, Qinhan Lv, Ruiqi Chen, Jing Yang, Yijia Fan, Xiaofei Sun, Jian Wang, Ziliang Chen, Liang Lin, and Keze Wang. Mm-cot: a benchmark for probing visual chain-of-thought reasoning in multimodal models, 2025. arXiv:2512.08228. 1

[64] Jusheng Zhang, Kaitong Cai, Jing Yang, Jian Wang, Chengpei Tang, and Keze Wang. Top-down semantic refinement for image captioning, 2025. arXiv:2510.22391. 1

[65] Jusheng Zhang, Kaitong Cai, Jing Yang, and Keze Wang. Learning dynamics of vlm finetuning, 2025. arXiv:2510.11978. 1

[66] Jusheng Zhang, Kaitong Cai, Qinglin Zeng, Ningyuan Liu, Stephen Fan, Ziliang Chen, and Keze Wang. Failure-driven workflow refinement, 2025. arXiv:2510.10035. 1

[67] Jusheng Zhang, Yijia Fan, Kaitong Cai, Zimeng Huang, Xiaofei Sun, Jian Wang, Chengpei Tang, and Keze Wang. Drdiff: Dynamic routing diffusion with hierarchical attention for breaking the efficiency-quality trade-off, 2025. 1

[68] Jusheng Zhang, Yijia Fan, Kaitong Cai, Xiaofei Sun, and Keze Wang. Osc: Cognitive orchestration through dynamic knowledge alignment in multi-agent llm collaboration, 2025. 1

[69] Jusheng Zhang, Yijia Fan, Kaitong Cai, and Keze Wang. Kolmogorov-arnold fourier networks, 2025. arXiv:2502.06018. 1

[70] Jusheng Zhang, Yijia Fan, Wenjun Lin, Ruiqi Chen, Haoyi Jiang, Wenhao Chai, Jian Wang, and Keze Wang. GAM-agent: Game-theoretic and uncertainty-aware collaboration for complex visual reasoning. In *The Thirty-ninth Annual Conference on Neural Information Processing Systems*, 2025. 1

[71] Jusheng Zhang, Yijia Fan, Zimo Wen, Jian Wang, and Keze Wang. Tri-MARF: A tri-modal multi-agent responsive framework for comprehensive 3d object annotation. In *The Thirty-ninth Annual Conference on Neural Information Processing Systems*, 2025. 1

[72] Jusheng Zhang, Xiaoyang Guo, Kaitong Cai, Qinhan Lv, Yijia Fan, Wenhao Chai, Jian Wang, and Keze Wang.

Hybridtoken-vlm: Hybrid token compression for vision-language models, 2025. arXiv:2512.08240. 1

[73] Jusheng Zhang, Zimeng Huang, Yijia Fan, Ningyuan Liu, Mingyan Li, Zhuojie Yang, Jiawei Yao, Jian Wang, and Keze Wang. KABB: Knowledge-aware bayesian bandits for dynamic expert coordination in multi-agent systems. In *Forty-second International Conference on Machine Learning*, 2025. 1

[74] Jensen Zhang, Ningyuan Liu, Yijia Fan, Zihao Huang, Qinglin Zeng, Kaitong Cai, Jian Wang, and Keze Wang. Llm-cas: Dynamic neuron perturbation for real-time hallucination correction, 2025. arXiv:2512.18623. 1

[75] Renrui Zhang, Jiaming Han, Chris Liu, Peng Gao, Ao-jun Zhou, Xiangfei Hu, Shilin Yan, Pan Lu, Hongsheng Li, and Yu Qiao. Llama-adapter: Efficient fine-tuning of language models with zero-init attention. *arXiv preprint arXiv:2303.16199*, 2023. 2

[76] Tianyi Zhang, Varsha Kishore, Felix Wu, Kilian Q. Weinberger, and Yoav Artzi. Bertscore: Evaluating text generation with BERT. *CoRR*, abs/1904.09675, 2019. 3

[77] Lianmin Zheng, Wei-Lin Chiang, Ying Sheng, Siyuan Zhuang, Zhanghao Wu, Yonghao Zhuang, Zi Lin, Zhuohan Li, Dacheng Li, Eric P. Xing, Hao Zhang, Joseph E. Gonzalez, and Ion Stoica. Judging llm-as-a-judge with mt-bench and chatbot arena. In *Proceedings of the 37th International Conference on Neural Information Processing Systems*, Red Hook, NY, USA, 2023. Curran Associates Inc. 1

[78] Chunting Zhou, Pengfei Liu, Puxin Xu, Srini Iyer, Jiao Sun, Yuning Mao, Xuezhe Ma, Avia Efrat, Ping Yu, Lili Yu, Susan Zhang, Gargi Ghosh, Mike Lewis, Luke Zettlemoyer, and Omer Levy. Lima: less is more for alignment. In *Proceedings of the 37th International Conference on Neural Information Processing Systems*, Red Hook, NY, USA, 2023. Curran Associates Inc. 2

[79] Yiyang Zhou, Chenhang Cui, Jaehong Yoon, Linjun Zhang, Zhun Deng, Chelsea Finn, Mohit Bansal, and Huaxiu Yao. Analyzing and mitigating object hallucination in large vision-language models. *arXiv preprint arXiv:2310.00754*, 2023. 1

[80] Jinguo Zhu, Weiyun Wang, Zhe Chen, Zhaoyang Liu, Shenglong Ye, Lixin Gu, Hao Tian, Yuchen Duan, Weijie Su, Jie Shao, Zhangwei Gao, Erfei Cui, Xuehui Wang, Yue Cao, Yangzhou Liu, Xinguang Wei, Hongjie Zhang, Haomin Wang, Weiye Xu, Hao Li, Jiahao Wang, Nianchen Deng, Songze Li, Yinan He, Tan Jiang, Jiapeng Luo, Yi Wang, Conghui He, Botian Shi, Xingcheng Zhang, Wenqi Shao, Junjun He, Yingtong Xiong, Wenwen Qu, Peng Sun, Penglong Jiao, Han Lv, Lijun Wu, Kaipeng Zhang, Huipeng Deng, Jiaye Ge, Kai Chen, Limin Wang, Min Dou, Lewei Lu, Xizhou Zhu, Tong Lu, Dahua Lin, Yu Qiao, Jifeng Dai, and Wenhui Wang. Internvl3: Exploring advanced training and test-time recipes for open-source multimodal models, 2025. 6

Self-Rewarded Multimodal Coherent Reasoning Across Diverse Visual Domains

Supplementary Material

6. Dataset Details

ScienceQA. ScienceQA is a multimodal multiple-choice dataset containing approximately 20k Question-Answer (QA) pairs. We derive the *ScienceQA-IMG* subset by filtering for instances that include image contexts. In this subset, each entry consists of an image, a question, and multiple candidate options, requiring Vision-Language Models (VLMs) to synergize visual perception with textual reasoning to derive the correct answer. During training, we utilize the full ScienceQA-IMG set but explicitly exclude the hint data provided in the original dataset. This exclusion compels the model to reason from scratch based solely on visual and textual inputs, thereby enhancing its independent problem-solving capabilities.

Visual7W. Visual7W is a dataset comprising 70k QA pairs with multiple-choice options, designed to evaluate object-level semantic understanding beyond simple local region recognition. We employ the complete Visual7W dataset for training to bolster the model’s semantic perception and fine-grained visual grounding abilities.

7. In-depth Analysis on Optimization and Efficiency

To rigorously validate the necessity of our reinforcement learning framework and assess its computational feasibility, we conducted two additional sets of experiments: (1) a comparison with Rejection Sampling Fine-Tuning (RFT) to verify the need for online optimization, and (2) a comprehensive training efficiency analysis.

7.1. Necessity of Online Optimization: SR-MCR vs. RFT

A critical question regarding the SR-MCR framework is whether the complex GRPO optimization is strictly necessary, or if simply filtering high-quality data using our proposed reward signals would suffice. To investigate this, we implemented a **Rejection Sampling Fine-Tuning (RFT)** baseline. Specifically, for each prompt in the training set, we sampled $N = 4$ responses using the base model π_0 , scored them using our unified self-reward R , selected the highest-scoring response, and fine-tuned the base model using standard Supervised Fine-Tuning (SFT).

Analysis. As shown in Table 4, while RFT yields a notable improvement over the base model (+3.9% on average), **SR-MCR significantly outperforms RFT** (+6.6% on average). This performance gap highlights a fundamental limitation of offline methods like RFT: they are strictly bound by the

Table 4. Necessity of Online Optimization. Comparison between the Base Model, Rejection Sampling Fine-Tuning (RFT), and our SR-MCR on the 7B scale. RFT uses the same 5-term reward to select the best-of- N ($N = 4$) samples for supervised training. SR-MCR significantly outperforms RFT, demonstrating the critical value of online exploration.

Method	Optimization	MMMU	MMBench	MME	V*Bench	Avg.	Δ
Qwen2.5-VL-7B (Base)	-	50.3	86.7	89.5	78.5	74.8	-
RFT-7B (Best-of- N)	Offline SFT	56.4	88.1	91.2	79.1	78.7	+3.9
SR-MCR-7B (Ours)	Online GRPO	67.6	91.2	94.5	80.6	81.4	+6.6

exploration capability of the *initial* policy. If the base model rarely generates a perfectly coherent reasoning chain for a complex query (e.g., in MMMU), RFT has no positive signal to harvest.

In contrast, SR-MCR employs **Online Policy Improvement**. Through iterative GRPO updates, the model’s distribution shifts dynamically during training, allowing it to explore reasoning paths that were initially low-probability but high-reward. This “exploration-exploitation” loop enables SR-MCR to solve complex tasks where the base model’s naive “best” answer is still suboptimal. Thus, the RL component is not over-engineering; it is essential for breaking the performance ceiling of the base model.

7.2. Training Efficiency and Computational Cost

One potential concern with SR-MCR is the overhead introduced by computing the five-component self-reward (involving DETR, DeBERTa, and CLIP) during training. We analyze the training efficiency in Table 5, comparing SR-MCR against standard SFT, PPO, and DPO. Experiments were conducted on $8 \times$ H800 GPUs with a global batch size of 128.

8. Generalization and Reward Mechanism Analysis

To further demonstrate the robustness of SR-MCR, we extend our evaluation along two critical dimensions: (1) cross-architecture generalization on different base models (InternVL2 and LLaVA-NeXT), and (2) a comparative analysis of our tool-based reward system versus LLM-based self-evaluation.

8.1. Cross-Architecture Generalization

A key question regarding the proposed framework is whether the hyperparameters and reward formulations are over-tuned for the Qwen2.5-VL architecture. To verify the universality of SR-MCR, we applied the exact same train-

Table 5. **Training Efficiency Analysis.** Comparison of training time (seconds per step), peak GPU memory usage, and performance gain on 7B models. While SR-MCR introduces overhead compared to SFT, it is significantly more efficient than PPO and achieves higher performance than DPO.

Method	Critic Model?	Reward Type	Time/Step (s)	Peak Mem (GB)	Avg. Acc (%)
SFT	✗	None	2.5	42	76.2
SR-PPO	✓	Neural	8.4	78	79.1
DPO	✗	Ref. Model	3.8	65	78.8
SR-MCR (Ours)	✗	Neural Tools	5.2	56	81.4

ing recipe (SR-GRPO with identical α, γ parameters) to two distinct open-source VLM architectures: **InternVL2-8B** and **LLaVA-NeXT-7B**.

Table 6. **Generalization Across Architectures.** We apply SR-MCR to InternVL2-8B and LLaVA-NeXT-7B without modifying hyperparameters. SR-MCR consistently improves performance across diverse architectures, confirming it is a general-purpose alignment recipe.

Base Model	Method	MMMU	MMBench	MME	V*Bench	Avg.	Δ
InternVL2-8B	Base	57.3	87.7	89.6	71.2	76.5	-
	SR-MCR (Ours)	61.8	89.4	92.1	74.5	79.5	+3.0
LLaVA-NeXT-7B	Base	52.1	84.3	87.4	68.9	73.2	-
	SR-MCR (Ours)	56.5	87.0	90.8	72.1	76.6	+3.4
Qwen2.5-VL-7B	SR-MCR (Ours)	67.6	91.2	94.5	80.6	81.4	+6.6

Analysis. As presented in Table 6, SR-MCR yields consistent performance gains across all tested architectures:

- **Universal Efficacy:** The method achieves a +3.0% average gain on InternVL2 and +3.4% on LLaVA-NeXT. Notably, improvements in V*Bench (+3.3% on InternVL2) highlight that the visual grounding reward \tilde{s}_{vis} (powered by CLIP/DETR) effectively transfers to models with different visual encoders (InternViT vs. CLIP-ViT-L).
- **Robustness of Cooling:** The stability of training on these models—without tuning the cooling temperature α —suggests that our reliability-weighted mechanism is robust to different logit scales and confidence distributions inherent in different base LLMs.

8.2. Ablation: External Tools vs. LLM-as-a-Judge

Our method relies on external tools (DETR, CLIP, NLI) to compute rewards. A natural alternative is to rely on the model’s own reflective capabilities (“LLM-as-a-Judge”) to self-evaluate its reasoning quality. We conducted an ablation where the unified reward R is replaced by a scalar score generated by the policy model itself via a self-evaluation prompt (e.g., “Rate the quality of your previous reasoning from 0 to 1”).

Deep Analysis: Why External Tools Matter? Table 7 reveals a critical insight: while Self-Reflection improves general reasoning (MMMU +4.9%), it **degrades** performance

on hallucination and grounding benchmarks (HallBench - 2.2%, V*Bench -0.7%). We attribute this divergence to the “*Self-Delusion*” phenomenon in RL fine-tuning:

- **Breaking the Hallucination Loop:** If a base model hallucinates an object (e.g., seeing a “cat” where there is none), its self-reflection module—sharing the same parameters—is highly likely to validate this hallucination as “correct.” This creates a positive feedback loop that reinforces errors. Our external **Object Detection Reward (DETR)** breaks this loop by providing an objective, model-agnostic ground truth surrogate. If DETR does not see a cat, the model is penalized, regardless of its confidence.
- **Objective vs. Subjective Signals:** LLM-as-a-Judge is subjective and prone to sycophancy. In contrast, our **CLIP-based Visual Grounding** and **NLI-based Consistency** signals offer stable, metric-driven rewards. The stark difference in HallBench performance (59.4 vs. 46.1) confirms that relying on external “eyes” is essential for grounding multimodal reasoning in reality, turning the “dependency on external tools” into a vital feature for reliability.

Analysis. The results in Table 5 reveal three key findings regarding the trade-off between cost and performance:

- **Speed vs. PPO:** While SR-MCR is slower than simple SFT (5.2s vs. 2.5s per step), it is **significantly faster than PPO (8.4s)**. This is because PPO requires maintaining and updating a separate Value (Critic) network, which effectively doubles the forward/backward passes. SR-MCR’s reward computation, although involving external models, is performed only in inference mode (no gradient computation) and is efficiently batched.
- **Memory Efficiency:** SR-MCR reduces Peak GPU Memory usage by **~28% compared to SR-PPO** (56GB vs. 78GB). By eliminating the Critic model, GRPO allows us to allocate more memory to larger batch sizes or longer context windows, which is crucial for multimodal reasoning tasks.
- **Inference Cost:** It is important to note that the overhead from DETR, CLIP, and DeBERTa exists **only dur**

Table 7. **Reward Source Comparison.** Comparison between our External Tool-based Reward and an Internal Self-Reflection Reward (LLM-as-a-Judge). External tools provide objective signals that significantly reduce hallucination (HallBench) and improve grounding (V*Bench), whereas self-reflection suffers from mode collapse.

Reward Mechanism	Signal Source	MMMU (Reasoning)	HallBench (Faithfulness)	V*Bench (Grounding)
Base Model	-	50.3	48.3	78.5
Self-Reflection SR-MCR (Ours)	Internal (Prompt) External Tools	55.2 (+4.9) 67.6 (+17.3)	46.1 (-2.2) 59.4 (+11.1)	77.8 (-0.7) 80.6 (+2.1)

ing training. The resulting SR-MCR model is architecturally identical to the base model, incurring **zero additional latency** during inference.

In summary, SR-MCR strikes an optimal balance: it accepts a manageable training overhead to leverage sophisticated, process-aware rewards that lightweight methods (like DPO) cannot easily incorporate, while avoiding the prohibitive costs of full Actor-Critic RL.

9. Prompts

To elicit structured and reflective reasoning, we design task-specific prompt templates tailored to the distinct formats of each benchmark:

- **MME:** Tailored for binary (Yes/No) questions, this template enforces a strict separation between the internal thought process (encapsulated within `<think>` tags) and the final verdict, ensuring a reflective reasoning stage before the conclusion.
- **V-Star:** Designed for complex multiple-choice questions, this prompt guides the model through a systematic three-step workflow: (1) analyzing the question and visual content, (2) evaluating each option against the evidence, and (3) conducting a critical review before concluding.
- **GPT-4o as a Judge:** Employed to quantitatively assess reasoning quality, this prompt instructs the evaluator to compare two Chain-of-Thought (CoT) responses, prioritizing the clarity, logic, and validity of the reasoning process over the mere correctness of the final answer.

MME Prompt Template

Your task is to answer the following yes/no question based on the provided image(s).

Inside the `<think>` tag, you must demonstrate a careful and reflective thought process.

After your thinking process, provide the final answer inside the `<answer>` tag. The answer must be **Yes** or **No**.

Question: {Question}

`<think>` [Your thought process here, clearly showing the three steps above.] `</think>`
`<answer>` {Answer} `</answer>`

V-Star Prompt Template

Your task is to answer the following multiple-choice question based on the provided image(s).

Inside the `<think>` tag, you must demonstrate a careful and reflective thought process following these steps: 1. **Analyze the Question and Image(s):** Break down the question, identify key information in the image(s), and determine what is being asked. 2. **Evaluate Each Option:** Systematically review each option. Provide reasoning for why an option is plausible or incorrect, referencing specific visual evidence and your knowledge. 3. **Critical Review and Final Conclusion:** Compare the options based on your analysis. State your final choice and provide a confident justification for why it is the best answer.

After your thinking process, provide the final answer inside the `<answer>` tag. The answer must be **only the letter** of the correct option (e.g., A, B, C, D).

Question: {Question}

`<think>` [Your thought process here, clearly showing the three steps above.] `</think>`
`<answer>` {Answer} `</answer>`

GPT-4o Prompt

You are a professional and impartial AI evaluation assistant. Your task is to carefully read the following question and two alternative 'Chain of Thought' (CoT) answers. You need to determine which Chain of Thought (Choice A or Choice B) is of higher quality, which is clearer, more logical, and more reasonable in its reasoning. Do not choose an answer solely because its final conclusion is correct; focus on evaluating the *reasoning process* itself. In your response, first analyze the strengths and weaknesses of both A and B, and then clearly state your final choice.

10. MME Performance Details

Figure 7 illustrates the performance of SR-MCR-7B across the MME benchmark. The model exhibits robust visual understanding, particularly in fine-grained tasks such as landmark, poster, and celebrity recognition. ACC measures the proportion of correctly answered yes-or-no questions, while ACC+ denotes the stricter metric where both questions for a given image must be answered correctly. The consistently strong results across diverse categories highlight SR-MCR-7B's ability to maintain high reasoning quality and prediction accuracy.

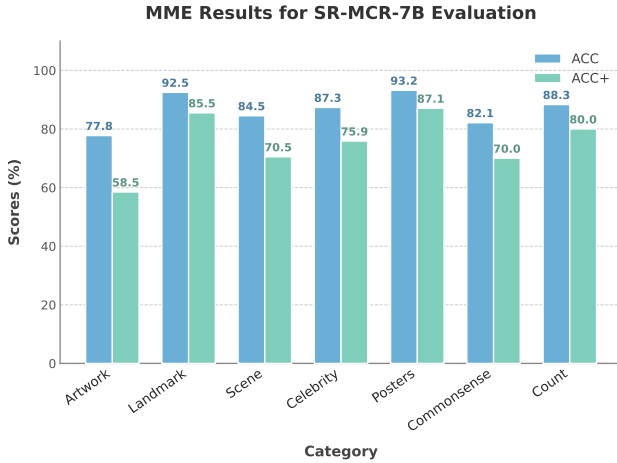


Figure 7. MME results for SR-MCR-7B across seven evaluation dimensions.

11. Theoretical Analysis: Gradient Properties and Noise Robustness

To theoretically substantiate the superiority of SR-MCR over baseline paradigms (Supervised Fine-Tuning and standard RL), we analyze the asymptotic properties of its gradient estimator. We demonstrate that SR-MCR provides a denser supervision signal than SFT via group-relative ranking and possesses an intrinsic noise-suppression property lacking in standard PPO due to our confidence-aware cooling mechanism.

11.1. Dense Supervision via Relative Advantage

Let the latent true reward distribution be $r(y|x, I)$. **Supervised Fine-Tuning (SFT)** or Rejection Sampling (RFT) effectively optimizes the log-likelihood of the single best-of- N sample, denoted as $y^* = \operatorname{argmax}_{y_i \sim \pi} r(y_i)$. The gradient approximation is:

$$\nabla_{\theta} \mathcal{J}_{\text{SFT}} \approx \mathbb{E}_{y^* \sim \pi_{\theta}} [\nabla_{\theta} \log \pi_{\theta}(y^*|x, I)] \quad (10)$$

Analysis of Gradient Sparsity: Theoretically, SFT approximates the reward landscape as a Dirac delta function

centered at y^* , i.e., $r(y) \approx \delta(y - y^*)$. This introduces two critical limitations: (1) **Information Loss**: It treats y^* as a ground-truth label (probability 1), discarding the valuable relative signals contained in suboptimal samples; (2) **High Bias**: It reinforces y^* even if y^* is merely a "lucky guess" or a local optimum, leading to potential overfitting.

In contrast, **SR-MCR (via GRPO)** optimizes the relative advantage within a sampled group $\{y_1, \dots, y_G\}$. The gradient estimator is defined as:

$$\nabla_{\theta} \mathcal{J}_{\text{SR-MCR}} \approx \frac{1}{G} \sum_{i=1}^G \underbrace{(R_{\text{adj}}(y_i) - \bar{R})}_{\text{Relative Advantage } \hat{A}_i} \nabla_{\theta} \log \pi_{\theta}(y_i|x, I) \quad (11)$$

Proof of Superiority: Unlike SFT, SR-MCR utilizes the *full distribution* of the generated group. Even a sample with mediocre quality contributes to the optimization: if a sample y_i is better than the group average \bar{R} (yet worse than y^*), it yields a positive signal ($\hat{A}_i > 0$); conversely, inferior samples provide negative gradients ($\hat{A}_i < 0$). This **fine-grained relative ranking** prevents the "mode collapse" often observed in SFT and drives the policy to continuously explore the upper bounds of the reward landscape.

11.2. Noise Robustness via Cooling Mechanism

A fundamental challenge in "Self-Reward" implies that the proxy reward $R(y)$ inherently contains noise ϵ (e.g., false positives from DETR or hallucinations in self-reflection). Standard RL algorithms (like PPO) blindly optimize this noisy signal, creating a risk of "reward hacking." We theoretically prove that our Cooling mechanism functions as a **Dynamic Variance Reducer**.

Recall our adjusted reward formulation: $R_{\text{adj}} = R(y) \cdot w_{\text{cool}}$, where $w_{\text{cool}} = \sigma(\kappa(c - l_{\theta}(y)))$ is the confidence-gated weight derived from the negative log-likelihood (NLL) $l_{\theta}(y)$.

Proposition 1 (Gradient Suppression under Uncertainty). Assume the reward estimation contains noise such that $R_{\text{proxy}} = R_{\text{true}} + \epsilon$. When the model hallucinates or exploits the reward model (reward hacking), the generation typically manifests as a statistical anomaly with high perplexity (high NLL $l_{\theta} \gg c$). As $l_{\theta}(y_i) \rightarrow \infty$, the cooling weight follows $w_{\text{cool}} \rightarrow 0$. Consequently, the norm of the gradient contribution is bounded:

$$\|\nabla_{\theta} \mathcal{J}_{\text{Cooling}}^{(i)}\| \leq w_{\text{cool}} \cdot \|\hat{A}_i \nabla_{\theta} \log \pi_{\theta}\| \xrightarrow{l_{\theta} \gg c} 0 \quad (12)$$

Interpretation: The cooling term acts as a differentiable "soft gate":

- **Case A (High Reward, High Uncertainty):** If $R(y_i)$ is high but the model is uncertain (indicating a potential hallucination or out-of-distribution reward hack), $w_{\text{cool}} \rightarrow 0$ effectively suppresses this gradient, preventing the policy from learning the noise.

Table 8. **Theoretical Comparison of Alignment Paradigms.** Comparison of gradient properties and resource requirements. SR-MCR occupies a unique sweet spot: it offers dense, process-level supervision similar to PPO but with the low memory footprint and intrinsic noise robustness lacking in standard RL methods.

Paradigm	Gradient Estimator	Supervision Signal	Noise Robustness	Critic Overhead	Granularity
SFT / RFT	$\nabla \log \pi(y^*)$	Sparse (Best-of- N)	Low (Overfits bias)	None	Outcome
PPO (RLHF)	$\hat{A}_t \nabla \log \pi(y_t)$	Dense (All samples)	Low (Prone to Hacking)	High	Outcome/Process
DPO	$\nabla \log \frac{\pi_\theta}{\pi_{ref}}$	Pairwise Relative	Medium (Implicit)	None	Outcome
SR-MCR (Ours)	$(R_{adj} - \bar{R}) \nabla \log \pi$	Dense (Group Relative)	High (via Cooling)	None	Process

- **Case B (High Reward, High Confidence):** If $R(y_i)$ is high and the model is confident ($l_\theta < c$), $w_{\text{cool}} \approx 1$, allowing full optimization strength.

This mechanism provides a theoretical guarantee that SR-MCR is robust against reward noise, applying a **soft trust-region constraint** based on generation confidence.

11.3. Theoretical Bound on Reward Hacking

We formally define the **Reward Hacking Region** \mathcal{H} as the subspace of generations where the proxy reward is deceptively high ($R(y) > \tau$) but the generation is statistically anomalous with respect to the truthful language manifold ($l_\theta(y) \gg c$).

Proposition 2 (Exponential Damping of Hacking Gradients). In SR-MCR, the gradient contribution from the hacking region \mathcal{H} is exponentially suppressed compared to standard Policy Gradient (PG).

Proof. Let $g_{\text{PG}}(y)$ be the standard gradient vector. The magnitude of the update in SR-MCR is scaled by the sigmoid cooling factor:

$$\|g_{\text{SR}}(y)\| = \sigma(c - l_\theta(y)) \cdot \|g_{\text{PG}}(y)\| = \frac{1}{1 + e^{-\kappa(c - l_\theta)}} \|g_{\text{PG}}(y)\| \quad (13)$$

For a hacking sample $y \in \mathcal{H}$ where $l_\theta(y) \rightarrow \infty$, the scaling factor decays exponentially:

$$\lim_{l_\theta \rightarrow \infty} \frac{\|g_{\text{SR}}(y)\|}{\|g_{\text{PG}}(y)\|} \approx e^{-\kappa l_\theta} \rightarrow 0 \quad (14)$$

This ensures that the policy update is strictly confined to the reliable region of the language model, theoretically preventing the catastrophic forgetting or mode collapse often triggered by reward hacking.

Discussion: The Bias-Variance Trade-off. It is worth acknowledging that the cooling mechanism introduces a bias by down-weighting low-confidence samples, even if they are factually correct. However, in the context of *Self-Reward*, where the reward signal stems from imperfect proxies (external tools), the *variance* of the gradient (driven by reward hacking and hallucinations) is the dominant factor destabilizing training. SR-MCR explicitly trades off a small degree of bias (ignoring potentially correct but

uncertain samples) for a significant reduction in variance. This ensures a monotonic improvement trajectory, preventing the model from collapsing into high-reward, low-quality modes.

12. Case Study

Table 10 and Table 11 illustrate success scenarios where SR-MCR-7B outperforms baselines. In Table 10, while Qwen2.5-VL struggles with color recognition and others fail to detect the object entirely, SR-MCR-7B accurately identifies the suitcase, demonstrating robust grounding. Similarly, Table 11 highlights our model’s precision in localizing a small-scale yellow car under challenging lighting, correctly inferring spatial relationships where competing methods falter.

However, limitations persist in specific challenging scenarios. As shown in Table 12 and Table 13, all evaluated models, including SR-MCR-7B, fail to provide correct answers. Table 12 reveals a susceptibility to context-induced hallucination, where models mistake a red toothbrush for blue due to the dominant clinical environment colors. Table 13 highlights difficulties in spatial reasoning under ambiguous perspectives, leading to consistent directional errors across all models.

13. Hyperparameters

Table 9 details the specific hyperparameters employed in our experiments.

Table 9. Hyperparameters used in the experiments.

Parameter	Value
<i>Data Configuration</i>	
Max Prompt Length	4096
Max Response Length	4096
<i>Algorithm (GRPO)</i>	
Disable KL	False
KL Coefficient	1.0×10^{-2}
Generations (n)	4
<i>Training Dynamics</i>	
Rollout Batch Size	4
Global Batch Size	4
Target Model Precision	BF16
Optimizer	AdamW
Learning Rate	1.0×10^{-6}
<i>Reward Function</i>	
Sentence Transformer	all-MiniLM-L6-v2
Target Length	1536

Table 10. Qualitative comparison on V*Bench (Attribute Recognition). The question asks for the color of a suitcase. **Correct Answer: D (brown).**

User Prompt	
Question: What is the color of the suitcase?	
Model	Reasoning & Output
Qwen2.5-VL-7B-Instruct	<p>The suitcase is located near the bottom right... <u>The color is not clearly distinguishable... appears to be dark... either black or brown.</u></p> <p>X Answer: C</p>
SAIL-VL2-8B-Thinking	<p><i>Got it, let's try to figure out the color... The options are red, gray, black, brown... Wait, maybe in the image, the suitcase is gray...</i></p> <p>X Answer: B</p>
VL-Rethinker-7B	<p><i>There are people standing near the entrance, but no suitcases are clearly visible in the image. ...</i></p> <p>X Answer: (No Answer)</p>
SR-MCR-7B (Ours)	<p><i>1. Analyze: Focus on the suitcase's appearance... 2. Evaluate: (d) "brown" indicates a specific shade that suggests a structured look. ... 3. Conclusion: A consistent tone suggests a deliberate design choice.</i></p> <p>✓ Answer: D</p>

Table 11. Qualitative comparison on V*Bench (Spatial Relationship)). The question asks for the position of a yellow car relative to a pool. **Correct Answer: A (left).**

User Prompt	
Model	Reasoning & Output
VL-Rethinker-7B	<p>Question: Is the yellow car on the left or right side of the pool?</p>  <p>Options: (A) left (B) right</p> <p><i>The yellow car appears to be situated on the right side of the pool... Thus, the spatial arrangement indicates the right side. ...</i></p> <p>X Answer: B</p>
WeThink-7B	<p><i>The yellow car is visible on the right side of the pool. ... Therefore, the yellow car is on the right side.</i></p> <p>X Answer: B</p>
Kimi-VL-A3B-Thinking	<p><i>... On the right side, near the edge of the pool, there's a yellow vehicle. ... So the answer should be the right side...</i></p> <p>X Answer: B</p>
SR-MCR-7B (Ours)	<p><i>1. Analyze: Identifying key objects... 2. Evaluate: The car is clearly positioned on the left side of the pool... 3. Conclusion: Option (A) is the correct choice.</i></p> <p>✓ Answer: A</p>

Table 12. Failure Case on V*Bench (Attribute Recognition). The question asks for the color of a toothbrush. **Correct Answer: D (red)**.

User Prompt	
Question: What is the color of the toothbrush?	
Options: (A) green (B) blue (C) yellow (D) red	
Model	Reasoning & Output
Qwen2.5-VL-7B-Instruct	<p>The dental office features light green cabinets... <u>The toothbrush inside the holder appears to have a handle that matches the teal/blue decor...</u> It is likely blue.</p> <p>X Answer: <u>B</u></p>
SAIL-VL2-8B-Thinking	<p><u>Scanning the room...</u> The environment is sterile with mint tones. <u>The object in the cup holder looks blueish under this lighting...</u> Not seeing any bright red objects.</p> <p>X Answer: <u>B</u></p>
VL-Rethinker-7B	<p><u>Focusing on the dental instruments...</u> <u>The toothbrush seems to be green or blue, blending with the tray.</u> No red toothbrush is clearly visible.</p> <p>X Answer: <u>A</u></p>
SR-MCR-7B (Ours)	<p>1. Analyze: Focus on the dental setting... 2. Evaluate: ... (b) “blue” suggests a possibility of a specific color associated with the setup... (d) “red” is less indicated... 3. Conclusion: ...consistent color scheme... indicates a specific color for dental tools.</p> <p>X Answer: <u>B</u></p>

Table 13. Failure Case on V*Bench (Spatial Relationship). The question asks for the position of a soccer ball relative to a bench. **Correct Answer: B (left).**

User Prompt	
Question: Is the soccer ball on the left or right side of the long bench?	
Options: (A) right (B) left	
Model	Reasoning & Output
Qwen2.5-VL-7B-Instruct	<p>The bench is located along the path. <u>From this angle, the soccer ball appears to be positioned on the right side of the bench structure...</u></p> <p>X Answer: A</p>
SAIL-VL2-8B-Thinking	<p><i>Locating the ball and the bench... The bench stretches along the right. The ball sits on the ground to the right of the bench's end... roughly aligned with the trees.</i></p> <p>X Answer: A</p>
VL-Rethinker-7B	<p><i>Analyzing spatial layout... The soccer ball is clearly visible on the right side relative to the bench... The perspective makes it appear further right.</i></p> <p>X Answer: A</p>
SR-MCR-7B (Ours)	<p><i>1. Analyze: Focus on the bench and surrounding elements. 2. Evaluate: (a) "right" does not indicate... (b) "left" suggests... 3. Conclusion: ...alignment with the bench's edge... indicates the ball's position relative to the bench.</i></p> <p>X Answer: A</p>